Pharmaceutical Analytical Chemistry Department[1], Faculty of Pharmacy, Chemistry Department[2], Faculty of Science, Beirut Arab University, Lebanon

Spectral and polarographic determination of eprosartan. Kinetic studies of the oxidation of eprosartan using a platinum electrode

F. A. El-Yazbi[1], H. H. Hammud[2], N. M. Sonji[1], G. M. Sonji[1]

Received December 7, 2007, accepted December 19, 2007

Dr. Ghassan Sonji, Pharmaceutical Analytical Chemistry Department, Faculty of Pharmacy, Beirut Arab University, 11-5020 Beirut, Lebanon
gmsonji@yahoo.com

Pharmazie 63: 420–427 (2008) *doi: 10.1691/ph.2008.7382*

Two simple and sensitive methods are presented for the determination of eprosartan in pharmaceutical preparations. The first method, spectrophotometry, was based on the oxidation of this drug by ammonium cerium (IV) nitrate in the presence of perchloric acid with subsequent measurement of the absorbance at 326 nm; this principle was adopted to develop a kinetic method for the determination of eprosartan in dosage forms. The second method, differential pulse polarography, was based on measuring the peak height at −1300 mV, corresponding to the reduction of the drug in Britton-Robinson buffer (pH 3). The proposed methods proved to be accurate and precise and can be applied for the routine analysis of this drug in commercial dosage forms, without interference from the excipients. The work was extended to study the electrochemical oxidation of eprosartan at different electrolysis currents (10–40 mA). The electrochemical decomposition products were characterized by UV/visible spectroscopy; the decomposition rates follow first order reactions and increase with raising the current. The degradation was found to be faster in basic than acidic medium. The thermodynamics for electrochemical decomposition were also evaluated at different pH values.

1. Introduction

Eprosartan (EPR) is an angiotensin II receptor antagonist widely used in the treatment of essential hypertension. This drug acts as a competitive blocker of angiotensin II type 1 receptors, preventing angiotensin from binding to its receptor, thereby blocking the vasoconstriction and the aldosterone-secreting effects of angiotensin II. Within the class of angiotensin II blockers, EPR is the only nonbiphenyl, nontetrazole antagonist. Its lack of metabolism by cytochrome P450 enzymes confers a low potential for metabolic drug interactions and may be of importance when treating elderly patients and those on multiple drugs. EPR has been demonstrated to be at least as effective in reducing blood pressure as the ACE inhibitor enalapril, and has significantly lower side effects and induce less cough, a side effect which may be related to bradykinin or other mediators such as substance P. In the recommended dose range 600 to 1200 mg once daily, EPR is safe and effective and well-tolerated in long-term treatment, either as monotherapy or in combination with other antihypertensive drugs such as hydrochlorothiazide (Ruilope and Jager 2003; Shusterman 1999).

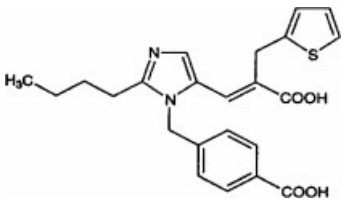

Eprosartan

Few methods have been reported for the analysis of this drug including micellar electrokinetic chromatographic method (Hillaert et al. 2003), capillary zone electrophoresis (Gonzalez et al. 2002) for its determination in dosage forms and HPLC methods for its quantitation in plasma (Lundberg et al. 1998; Ferreiros et al. 2006).

The present work utilized spectrophotometric and voltammetric techniques for the determination of EPR in dosage forms.

Organic sulfides can be oxidized to the sulfoxides and then to the sulfones (El Yazbi and Blaih 1993). This oxidation can be carried out by ammonium cerium(IV) nitrate. Being primary standard, Ce(IV) has been used for quantitative determination of some sulfur containing compounds (El Yazbi et al. 2003) due to its high oxidation potential and excellent solution stability in acidic medium. Its acidic solution is yellow in color, while its reduced form is colorless. Therefore, a kinetic spectrophotometric method was developed for EPR determination in pure form and pharmaceutical formulations. The method was based on the reaction of the drug with Ce(IV) in perchloric acid medium at room temperature. The reaction was followed spectrophotometrically by measuring the increase in absorbance at 326 nm as a function of time.

In the polarographic method, EPR solution in Britton-Robinson buffer (pH 3) – ethanol (1 : 4), was subjected to differential pulse polarographic measurements using a hanging mer-

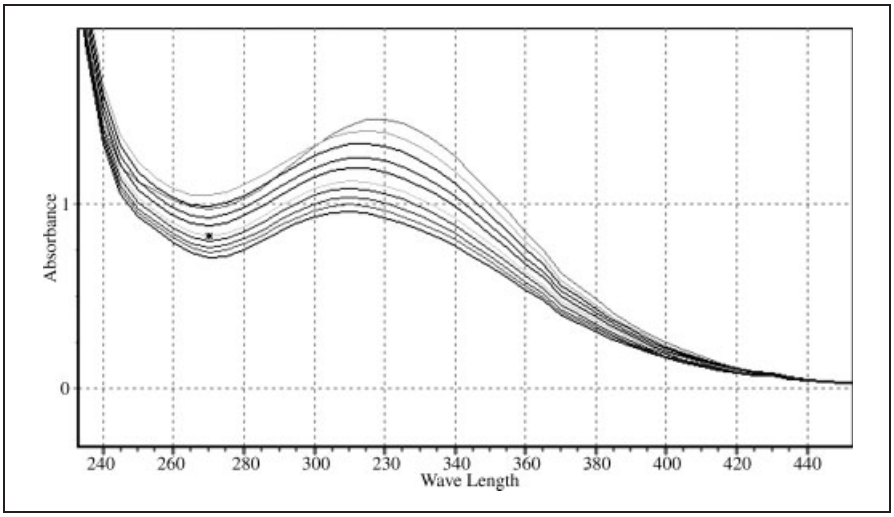

Fig. 1:
Differential absorption spectra of Ce(IV) consumed through oxidation of 12 μg/ml EPR vs time

cury electrode (HME), where the peak height at −1.30 V corresponding to EPR reduction has been used for its selective determination.

The work was also extended to detect the degradation process of EPR, using platinum electrodes either in KCl medium or buffer solutions at different pHs 4.0, 7.0, 8.5 in a separate cell compartment at different temperatures and various current intensities.

2. Investigations, results and discussion

2.1. Spectrophotometric method

Cerium(IV) was used extensively as strong oxidant for the determination of some organic compounds. Due to its high oxidation potential and excellent solution stability, this reagent has been utilized to develop a quantitative method for the analysis of EPR in dosage forms. The method depends on measuring the absorbance of the consumed Ce(IV) at 326 nm. This was achieved by measuring the absorbance of a blank containing solution of certain concentration of Ce(IV) against the test containing the same concentration of this reagent (Fig. 1). The redox reaction was completed within 60 min. The maximum absorbance obtained, remained stable for at least 30 min. The different conditions affecting the reaction were extensively studied so as to furnish the best sensitivity, stability and adherence to Beer's law. It was found that acid medium is needed to prevent precipitation of hydrated cerric oxide. Ce(IV) is not readily soluble in water, but becomes stable when dissolved in 0.5 M sulphuric acid. However, the reaction of EPR and Ce(IV) was found to proceed quantitatively only in presence of 1 M perchloric acid.

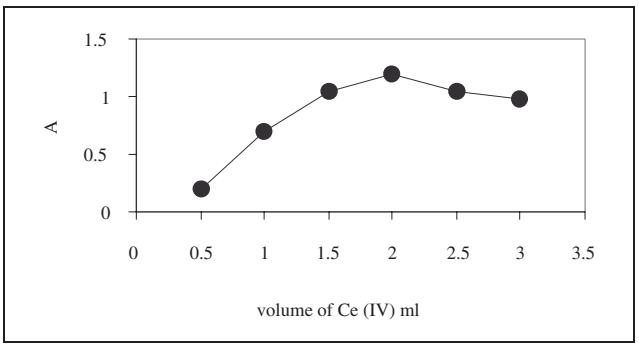

Fig. 2: Effect of Ce(IV) volume (2×10^{-3} M) on the absorbance measurement of 15 μg/ml EPR with Ce(IV)

In case of other acids as sulphuric or nitric acid non-stoichiometric reaction was obtained. Concerning Ce(IV) concentration, the results showed that as the concentration of Ce(IV) was increased the absorbance difference readings were increased to give a maximum absorption at 2 ml of 2×10^{-3} M solution, after which the signals started to decrease (Fig. 2).

As the intensity of color increases with time, it was useful to develop a kinetically based method for the assay of EPR. The rate of the reaction was also found to be EPR-dependent. The rates were followed at room temperature with various concentrations of EPR in the range 5–14 μg/ml, keeping Ce(IV) and perchloric acid concentrations constant. It was found that the reaction rate obeys the following equation:

$$\text{Rate} = K'[\text{EPR}]^n \qquad (1)$$

Where K' is the pseudo-order rate constant and n is the order of the reaction. The rate could be estimated as $\Delta A/\Delta t$, where A is the absorbance and t the time in seconds. Taking the logarithms of rates and concentrations (Table 1), Eq. (1) is transformed into:

$$\log(\text{rate}) = \log(\Delta A/\Delta t) = \log K' + n \log[\text{EPR}] \qquad (2)$$

Regression of log (rate) versus log [EPR] gave the regression equation

$$\log(\text{rate}) = 1.115 + 0.9993 \log[\text{EPR}] \qquad r = 0.999$$

Hence $K' = 13.03\ \text{sec}^{-1}$ and the reaction is pseudo-first order ($n = 1.115 \approx 1$) with respect to EPR.

Under the optimum experimental conditions stated previously, the course of the reaction of EPR and Ce(IV) was followed spectrophotometrically at 326 nm. The initial rates of reaction were determined from the slopes of the initial tangent to the absorbance-time curves at different concentrations of the drug. Calibration curves of absorbance versus concentration of EPR were plotted at fixed

Table 1: Logarithms of rates of different concentrations of EPR at room temperature at 326 nm

log ΔA/Δt	log [EPR]
−4.446	−5.558
−4.2236	−5.336
−4.019	−5.132
−3.923	−5.035

times, and the regression equations were calculated. The slope increases with time and the most acceptable value of correlation coefficient and intercept were obtained for a fixed time of 60 min, which was recommended as the most suitable time interval for the assay of EPR in pharmaceutical formulations.

2.2. Voltammetric method:

Differential pulse polarography using a hanging mercury electrode was applied for the determination of EPR in buffer solutions of pH 2–12. The compound gave a single reduction peak corresponding to the reduction of −C=N− center. In (1 : 4) mixture of Britton-Robinson-buffer pH 3: ethanol, the differential pulse polarograms displayed reproducible peaks at Ep −1300 mV versus Ag/AgCl. Under these conditions linearity between EPR concentration and peak height was observed in $0.56–3.28 \times 10^{-5}$ M concentration range (Fig. 3).

The mechanism involves two electron reduction of the imine group (Scheme).

This mechanism is supported by the observed shift of Ep towards negative potential with the rise in pH up to 4, (Hammud et al. 2006; Jain and Jain 1994; El-Hallag et al. 1994). The change in Ep with respect to pH calculated from the experimental data: ΔEp/ΔpH (mV/pH unit) = 50. When the basic form of EPR predominates at high pH (6–12), Ep remains unchanged.

The linearity of the proposed methods was tested by applying the methods to synthetic solutions containing the commonly used excipients to which different concentrations of EPR have been added above and below the normal levels expected in the sample. The graphs obtained by plotting the absorbance of consumed Ce(IV) versus EPR concentration in the range stated in Table 2 for the spectrophotometric method, and the polarogram peak height versus EPR concentration in the range stated also in Table 2 for the voltammetric method, exhibited linear relationships. The good linearity of the calibration graph was clearly evident from the values of the correlation coefficient and the small values of standard error of intercept or slope at regression line.

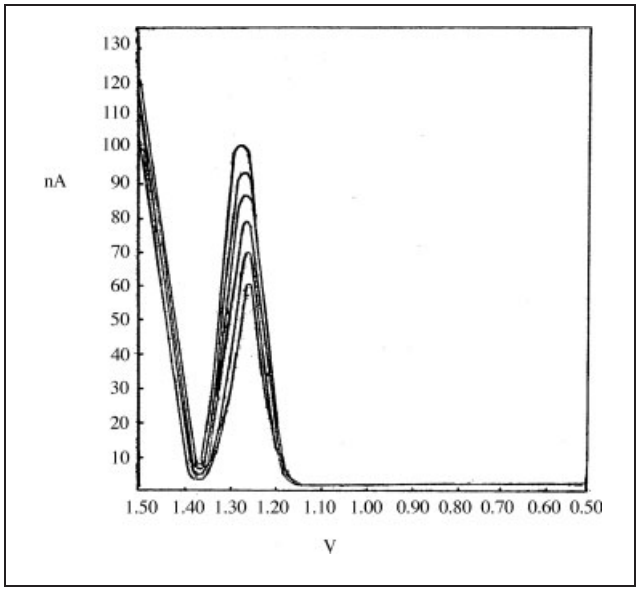

Fig. 3: Differential pulse polarograms of EPR (0.56, 1.11, 1.66, 2.21, 2.75, and 3.28) $\times 10^{-5}$ M in B.R. buffer pH 3: ethanol (1 : 4) versus Ag/AgCl (KCl 3M) reference electrode

Scheme

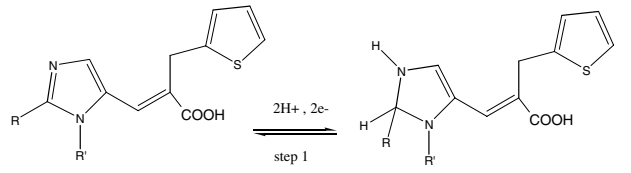

The accuracy of the proposed methods was tested by calculating the recoveries of the drug, at five levels below and above the ratio labeled in the pharmaceutical tablets. Good recoveries were obtained, indicating no interference from excipients (Table 2).

The precision of the proposed methods was evaluated by determining the relative standard deviation of the assay results of three different concentrations, each in three replicates. The results obtained in Table 2 showed that the relative standard deviation was less than 2% which indicated the high precision of the assay.

The limits of detection (LoD) and quantitation (LoQ) were calculated using the equations:

$$\text{LoD} = \text{B} + 3\,\text{s} \quad \text{and} \quad \text{LoQ} = \text{B} + 10\,\text{s}$$

where s and B are the standard deviation and the mean of 10 independent sample blank values. The values of LoD and LoQ are stated in Table 2.

The proposed methods were applied for the analysis of EPR in its dosage form. The results obtained were precise and accurate, and indicated the potential for adapting these methods for the assay of EPR in dosage forms.

Table 2: Validation data for the determination of EPR by the proposed methods

Parameters	UV method	Voltammetric method
	λ (nm) 326	Ep (mV) − 1300
Regression equation	*y = 0.83285 X − 0.10972	**y = −30.25 X − 0.488
r[a]	0.9968	0.9997
S1[b]	0.0015	0.265
S2[c]	1.484×10^{-3}	6×10^{-4}
Linearity Range (μg ml^{-1})	5.0–14	2.0–14
Accuracy (Mean ± SD)	100.51 ± 0.9821	99.94 ± 0.52
Precision (RSD %)	0.98	0.52
LoD	4.319×10^{-3}	3.251×10^{-4}
LoQ	8.015×10^{-3}	7.542×10^{-4}

* Where X is the concentration of EPR (μg ml^{-1}); y is the absorbance of consumed Ce(IV) at 326 nm.
** Where X is the concentration of EPR (μg ml^{-1}); y is the polarogram peak height at Ep −1300 mV.
a: The coefficient of correlation
b: Standard error of intercept at regression line
c: Standard error of slope at regression line

2.3. Kinetic studies of EPR electrochemical decomposition

We have used bulk electrolysis in order to study the electrochemical decomposition of EPR in separate compartment using two platinum electrodes (Hammud et al. 2006).

The equation $\mathrm{Ln\ A = Ln\ A_0 - kt}$ was applied in order to calculate the rate constant of electrodecomposition k ($\mathrm{min^{-1}}$). Where A is the absorbance at λ_{max} of EPR remaining after time t (min) of electrolysis and A_0 is the absorbance of initial EPR. The obtained products do not absorb at λ_{max} of EPR. First-order curves were fitted to the Ln A vs t data at different electrolysis currents i (mA), (Fig. 4). The resulting apparent first order rate constant k is reported in Table 4. Also reported is R^2 as a measure of goodness in the fit. The data also indicates that k ($\mathrm{min^{-1}}$) increases linearly with electrolysis current i (mA) according to equation $k = ai + c$, (Fig. 5).

The absorbance spectra versus λ_{max}(nm) of electrolysis of EPR (7×10^{-5} M) at different time are plotted in Figs. 6–8 at i = 30 mA and at different pH. The rate constant k ($\mathrm{min^{-1}}$) at 25 °C of electro-decomposition of EPR (7×10^{-5} M) at i = 30 mA in non buffered 25% ethanol solution (KCl 0.134 M, pH 4.50) was found to be 0.0243 $\mathrm{min^{-1}}$.

To investigate the mechanism of electrochemical decomposition of EPR at different pH and evaluate thermodynamic parameters, the experimental conditions such as pH and conductivity have been measured at the start and end of experiment. Large shift in pH was obtained, where the pH decreased chiefly in both unbuffered [25% ethanol and KCl (0.134 M)] and buffered solutions, (Table 3). However, the shift in conductivity was negligible.

The mechanism of electrochemical decomposition involves oxidation of EPR when it was placed in an anode compartment. Absorbance spectra versus time for electro-decomposition of EPR in an anode compartment was recorded for the acidic form at pH 4.0 (Fig. 6) and for the basic form at pH 7.0 (Fig. 7) and pH 8.5 (Fig. 8). The imine group absorption peak in the region (280–295 nm)

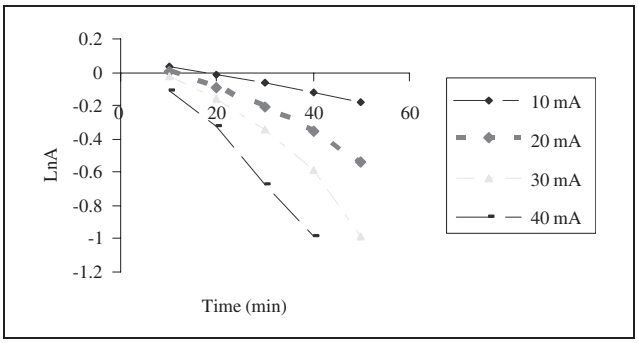

Fig. 4: Electro-decomposition of EPR (7×10^{-5} M) at pH 4.6 in an anode compartment using different currents (mA) at 25 °C

Table 3: pH and conductivity change during electrolysis of EPR in an anode compartment at 25 °C and current i = 30 mA

Medium	Initial		Final	
	pH	Conductivity (mS/cm)	pH	Conductivity (mS/cm)
KCl	4.5	8.74	2.21	11.39
	4.3	9.64	2.40	10.87
Buffer	7.0	10.13	3.03	10.77
	8.5	9.77	5.78	9.29

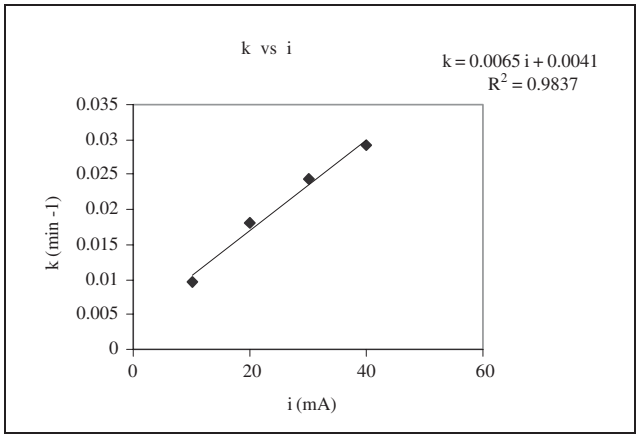

Fig. 5: Variation of the rate constant K ($\mathrm{min^{-1}}$) of EPR electro-chemical decomposition with electrolysis current (mA) in an anode compartment

decreases with time for both forms of EPR. This also implies that oxidation occurred at imine group resulting in loss in conjugation in the product. But no complete oxidation of CO_2 of EPR was obtained at these conditions.

Our polarographic studies show that EPR is reduced into amines at the mercury electrode (Scheme). However, bulk electrolytic reduction of EPR was not observed at the cathode compartment with Pt electrode (i = 30 mA) in 25% ethanol–KCl (0.134 M). Only change of EPR from acidic form ($\lambda_{max} = 280$ nm) to basic form ($\lambda_{max} = 295$ nm) was obtained in unbuffered solution. This implies that electrochemical reduction occurs for hydrogen instead of EPR due to low over-potential of hydrogen evolution (Adams 1969).

The electrochemical decomposition rate data of EPR (7×10^{-5} M) in an anode compartment (i = 30 mA) at 25 °C and different pH were plotted as Ln A versus time (min). First-order curve was fitted to the data. The apparent first order rate constant, k, is reported at different temperatures with or without buffer for electrolysis (Tables 4–8). It was found that the rate constant of electrodecomposition of EPR (basic form) at pH 8.5 was greater than that of the acidic form: k (pH 4.0) < k (pH 7.0) < k (pH 8.5).

Comparison of the fraction of EPR remaining (C_t/C_0) versus electrolysis time t (min) in anode compartment for acidic and basic forms is shown in Fig. 9. This can be due to the difficulty of the acidic species to undergo oxidation.

The thermodynamic parameters associated with the electro-decomposition of EPR were calculated as follows (Hammud et al. 2006).

Plot of ln k vs 1/T gives the value of activation energy Ea according to the Arrhenius equation:

$$\ln k = -\frac{E_a}{R \cdot T} + \ln A \qquad (3)$$

The activation enthalpy $\Delta H^{\neq}$ can be calculated from E_a at each temperature using:

$$E_a = \Delta H^{\neq} + R \cdot T \qquad (4)$$

The $\Delta H^{\neq}$ value can also be calculated from the slope of the plot of ln k/T vs 1/T by the use of Eyring equation:

$$\ln \frac{k}{T} = -\frac{\Delta H^{\neq}}{R} \cdot \frac{1}{T} + \ln \frac{k_B}{h} + \frac{\Delta S^{\neq}}{R} \qquad (5)$$

The intercept gives the value of activation entropy $\Delta S^{\neq}$ according to:

$$y(x = 0) = \ln \frac{k_B}{h} + \frac{\Delta S^{\neq}}{R} \qquad (6)$$

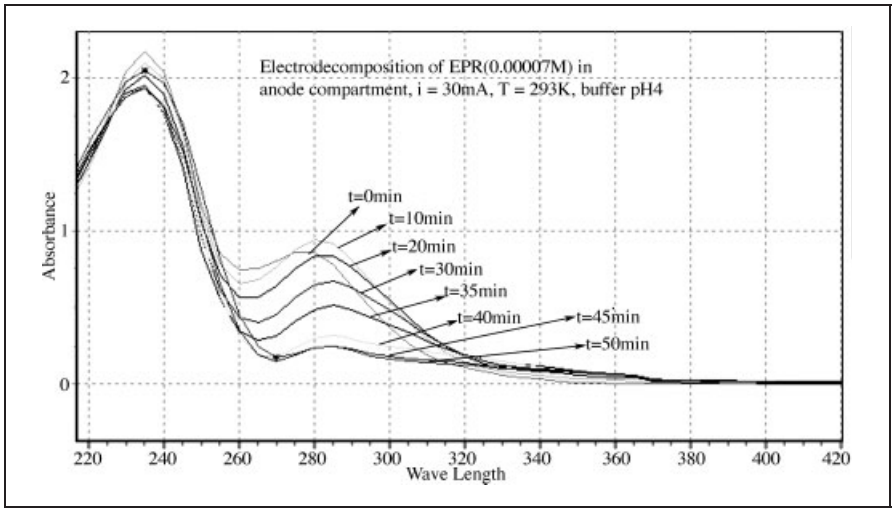

Fig. 6:
Absorbance spectra vs λ (nm) at different time of electrolysis of EPR (7×10^{-5} M), pH 4.0 in an anode compartment, i = 30 mA and t = 20 °C. EPR (Acidic form $\lambda_{max} = 285$ nm)

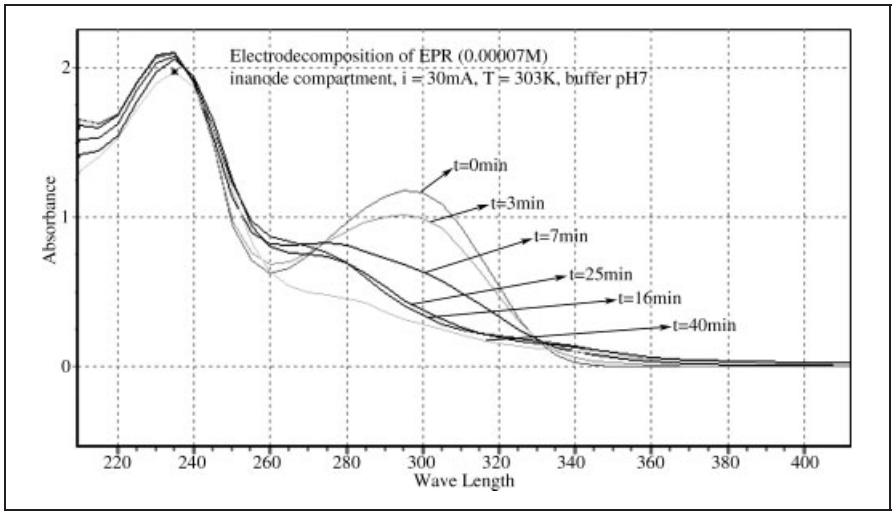

Fig. 7:
Absorbance spectra vs λ (nm) at different time of electrolysis of EPR (7×10^{-5} M), pH 7.0 in an anode compartment, i = 30 mA and t = 30 °C. EPR (Basic form $\lambda_{max} = 295$ nm)

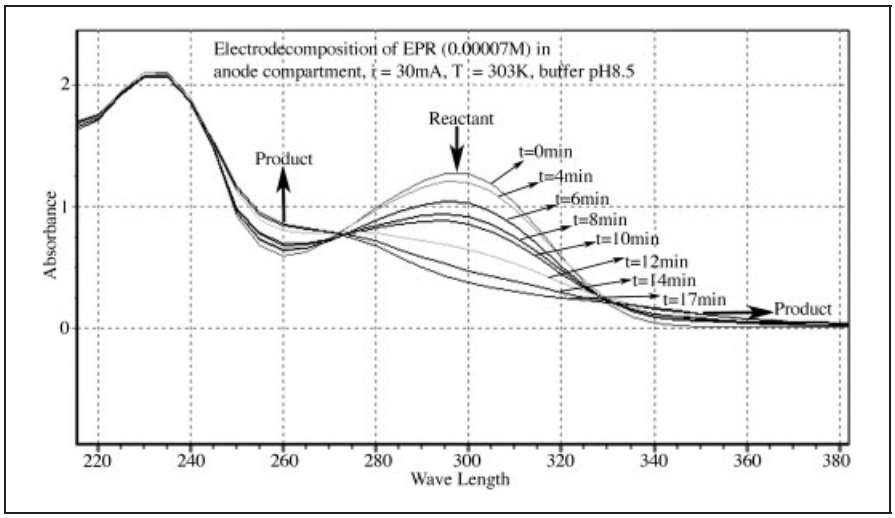

Fig. 8:
Absorbance spectra vs λ (nm) at different time of electrolysis of EPR (7×10^{-5} M), pH 8.5 in an anode compartment, i = 30 mA and t = 30 °C. λ_{max} of basic form of reactant EPR = 295 nm, λ_{max} of oxidation product = 270 nm)

Where k_B = Boltzmann's constant $[1.381 \times 10^{-23}\ J \cdot K^{-1}]$ and h = Plank constant $[6.626 \times 10^{-34}\ J \cdot s]$
The free activation enthalpy $\Delta G^{\neq}$ is equal to:

$$\Delta G^{\neq} = \Delta H^{\neq} - T \cdot \Delta S^{\neq} \quad (7)$$

k values as well as E_a, $\Delta H^{\neq}$, $\Delta S^{\neq}$ and $\Delta G^{\neq}$ values for electro-decomposition of EPR in an anode compartment are reported in Tables 5–8.

Figure 10 is an example of plot of LnK vs 1/T where E_a value was calculated from the slope. Figure 11 is an example of plot of LnK/T vs 1/T; the value of $\Delta H^{\#}$ was obtained from the slope while that of $\Delta S^{\#}$ was calculated from the intercept.
The thermodynamic values for the electrochemical decomposition parameters E_a, $\Delta H^{\#}$, $\Delta S^{\#}$ and $\Delta G^{\#}$ showed variations between acidic and basic forms (Tables 4–8). This

Table 4: Rate constants k (min^{-1}) of the electro-decomposition of EPR (7×10^{-5} M) in an anode compartment, in 25% ethanol-KCl (0.134 M) (pH = 4.5) using different electrolysis currents at 25 °C, and the R^2 values of the fit of the first order curves LnAvst

Current (mA)	k $(min)^{-1}$	R^2
10	0.0096	0.8720
20	0.0181	0.9179
30	0.0243	0.8435
40	0.0291	0.9253

was due to different decomposition mechanisms for both forms. The negative values of $\Delta S^{\#}$ in all cases indicate that the oxidative electrochemical-decomposition does not cause disproportionation of EPR. Also $\Delta S^{\#}$ values for the basic form (pH 8.5) were more negative than those of the acidic form (pH 4.3), while $\Delta H^{\#}$ for acidic species were more positive than basic species. E_a for basic form was smaller than basic form indicating faster reaction and larger k value was obtained.

3. Experimental

3.1. Instrumentation

Computerized OPTIMA SP-3000 UV-Visible spectrophotometer. The absorption spectra were measured using 1 cm quartz cells. Metrohm 626 Polarecord with a model 663 VA Stand assembly containing a multimode electrode (used in the dropping and hanging drop electrode modes) as working electrode, a carbon electrode as auxiliary electrode and a reference Ag/AgCl (3M KCl) electrode. PHYWE power supply with a potential range 0–250 V, Two platinum electrodes 0.25 mm thick, an amperometer. Precisterm thermostated water bath.

3.2. Materials and reagents

All solvents and chemicals were of analytical grade. Ammonium ceric nitrate (Fluka Chemie GmbH, Switzerland), was prepared as 2×10^{-2} M in 0.5 M sulphuric acid, and then further dilution with 1 M perchloric acid to obtain 2×10^{-3} M of Cerium IV. Britton-Robinson buffer pH 3: 0.04 M

Table 5: Rate constants and thermodynamic data for electrochemical oxidation of EPR (7×10^{-5} M) in an anode compartment in 25% ethanol-KCl medium (0.134 M), pH = 4.50 at i = 30 mA, (acidic form, Abs_{meas} at $\lambda = 275$ nm)

T (K)	k (min^{-1})	Ea $(KJ \cdot mol^{-1})$	$\Delta H^{\#}$ (1)[a] $(KJ \cdot mol^{-1})$	$\Delta H^{\#}$ (2)[b] $(KJ \cdot mol^{-1})$	$\Delta S^{\#}$ $(J \cdot mol^{-1} \cdot K^{-1})$	$\Delta G^{\#}$ $(KJ \cdot mol^{-1})$
293	0.0235	4.63	2.19	2.13	−302.559	90.78
298	0.0243		2.15			92.29
303	0.0250		2.11			93.81
308	0.0258		2.07			95.32

a: from Arrhenius equation, b: from Eyring equation

Table 6: Rate constants and thermodynamic data for electrochemical oxidation of EPR (7×10^{-5} M) in an anode compartment in 25% ethanol buffered medium (pH 4.0), at i = 30 mA, (acidic form, Abs_{meas} at $\lambda = 285$ nm)

T (K)	k (min^{-1})	Ea $(KJ \cdot mol^{-1})$	$\Delta H^{\#}$ (1)[a] $(KJ \cdot mol^{-1})$	$\Delta H^{\#}$ (2)[b] $(KJ \cdot mol^{-1})$	$\Delta S^{\#}$ $(J \cdot mol^{-1} \cdot K^{-1})$	$\Delta G^{\#}$ $(KJ \cdot mol^{-1})$
293	0.0297	12.38	9.95	9.89	−274.22	90.24
298	0.0317		9.91			91.61
303	0.0346		9.86			92.98
308	0.0380		9.82			94.35

a: from Arrhenius equation, b: from Eyring equation

Table 7: Rate constants and thermodynamic data for electrochemical oxidation of EPR (7×10^{-5} M) in an anode compartment in 25% ethanol buffered medium (pH = 7.0) at i = 30 mA, (basic form, Abs_{meas} at $\lambda = 295$ nm)

T (K)	k (min^{-1})	Ea $(KJ \cdot mol^{-1})$	$\Delta H^{\#}$ (1)[a] $(KJ \cdot mol^{-1})$	$\Delta H^{\#}$ (2)[b] $(KJ \cdot mol^{-1})$	$\Delta S^{\#}$ $(J \cdot mol^{-1} \cdot K^{-1})$	$\Delta G^{\#}$ $(KJ \cdot mol^{-1})$
293	0.043	27.98	25.55	25.49	−217.74	89.29
298	0.052		25.51			90.38
303	0.067		25.47			91.47
308	0.073		25.42			92.55

a: from Arrhenius equation, b: from Eyring equation

Table 8: Rate constants and thermodynamic data for electrochemical oxidation of EPR (7×10^{-5} M) in an anode compartment in 25% ethanol buffered medium (pH = 8.50) at i = 30 mA, (basic form, Abs_{meas} at $\lambda = 295$ nm)

T (K)	k (min^{-1})	Ea $(KJ \cdot mol^{-1})$	$\Delta H^{\#}$ (1)[a] $(KJ \cdot mol^{-1})$	$\Delta H^{\#}$ (2)[b] $(KJ \cdot mol^{-1})$	$\Delta S^{\#}$ $(J \cdot mol^{-1} \cdot K^{-1})$	$\Delta G^{\#}$ $(KJ \cdot mol^{-1})$
293	0.0642	4.364	1.93	1.87	−295.10	88.33
298	0.0663		1.89			89.81
303	0.0684		1.85			91.28
308	0.0700		1.81			92.76

a: from Arrhenius equation, b: from Eyring equation

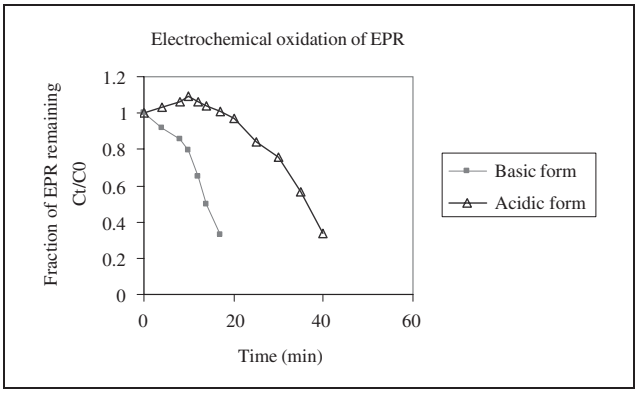

Fig. 9: Comparison of the fraction of EPR remaining (C_t/C_0) vs time of electrolysis t (min) (7×10^{-5} M) in an anode compartment with i = 30 mA, for acidic form (buffer pH = 4.0) and basic form (buffer pH = 8.5) at 20 °C

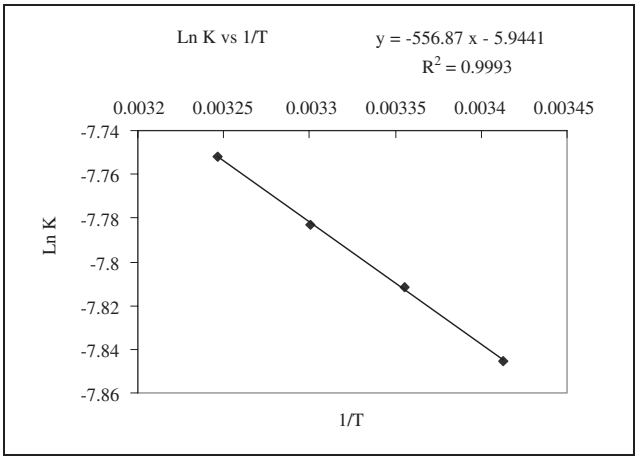

Fig. 10: Plot of LnK vs. 1/T for EPR (7×10^{-5} M) in KCl (0.134 M) at pH 4.6

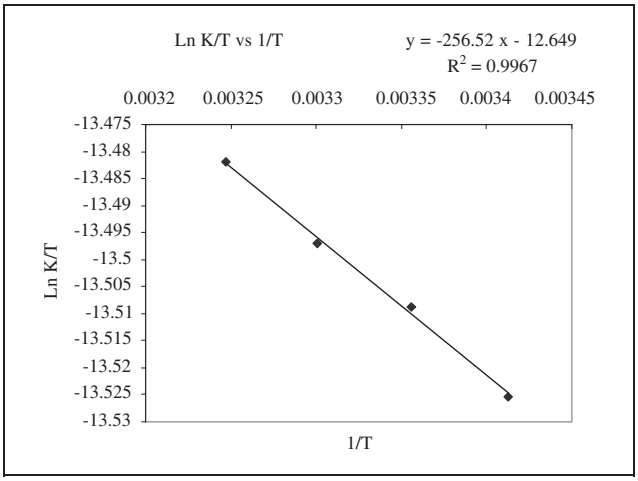

Fig. 11: Plot of LnK/T vs. 1/T for EPR (7×10^{-5} M) in KCl (0.134 M) at pH 4.6

acetic acid, 0.04 M H_3PO_4, 0.04 M H_3BO_3 and 0.2 N NaOH. Teveten® tablets (Solvay Pharmaceuticals B.V., The Netherlands). Each tablet was labeled to contain 600 mg eprosartan.

3.3. Standard solutions

3.3.1. Spectrophotometric method

Standard solution of EPR (6 mg · ml^{-1}) was prepared in ethanol. An aliquot was then diluted with 0.1 N HCl to give a solution of 0.12 mg · ml^{-1}.

3.3.2. Polarographic method

Stock solution of EPR containing 1.4×10^{-3} M was prepared in ethanol. Standard EPR solutions of (0.56, 1.11, 1.66, 2.21, 2.75, and 3.28) $\times 10^{-5}$ M were then prepared in (1 : 4) mixture (Britton-Robinson buffer pH 3: ethanol).

3.3.3. Electrochemical decomposition

Solutions studied contain EPR (7×10^{-5} M) and KCl (0.134 M) in 25% ethanol-water mixture with or without Britton Robinson buffer (0.004 M) at pH 4.0, 7.0 and 8.5.

3.4. Calibration graphs

3.4.1. Spectrophotometric method

Aliquot portions of the standard solution, within the concentration range 5–14 μg/ml, were transferred into a set of 10 ml volumetric flasks, and then 2 ml of Ce(IV) was added. The contents of each flask were mixed well, completed to the mark with distilled water and left to stand for 60 min at room temperature. The absorbance of the blank was measured against each solution at 326 nm.

3.4.2. Polarographic method

Aliquots of the standard solution, within the concentration range 2–14 μg/ml, were mixed thoroughly in the electrochemical cell with 20 ml ethanol and 5 ml Britton-Robinson buffer pH 3, purged with pure nitrogen for 10 min. The differential pulse polarographic measurements were performed with potential scan rate 5–10 mV/s, with measurement of 1 nA/mm for current and 50 mV/cm pulse for potential. The polarogram was recorded from 0 to −1500 mV (Fig. 3).

3.4.3. Electrochemical decomposition

The experimental apparatus consists of 1) a power supply potential range (0–250 V) 2) two platinum electrodes 0.25 mm thick 3) a thermostat water bath and 4) an amperometer. The electrochemical decomposition of EPR has been carried out at different voltages using two platinum electrodes in an anode compartment with a counter electrode.

EPR solutions (7×10^{-5} M) were prepared in 25% ethanol-water mixture in presence of KCl (0.134 M) with or without Britton-Robinson buffer (0.004 M) at pH 4.0, 7.0 and 8.5. The counter electrode compartment contained KCl (0.134 M). One experiment was done at 25 °C with different applied voltages (12–45 V) corresponding to electrolysis currents (10–40 mA) in KCl medium (pH 4.5). The second experiment was done at an electrolysis current 30 mA at various temperature 20, 25, 30, 35 °C. The starting solutions pHs were 4.0–8.5. The pH and conductance of solution was measured before and after the experiment. In most cases the pH decreased while conductance remained almost unchanged (Table 3).

In a typical experiment, aliquot portions of EPR solutions were placed in the anode compartment. The rate of the reaction was followed by measuring UV-Visible absorbance spectra of EPR using a SP-3000 OPTIMA UV-Visible spectrophotometer. The absorbance at λ_{max} of EPR versus time was used for calculation of rate constant.

3.5. Assay of drug in tablets

An amount of powdered tablets equivalent to 600 mg of the drug was transferred into a 100 ml volumetric flask, dissolved in ethanol by sonication for 30 min, completed to volume with the same solvent mixed well and filtered. A 2 ml aliquot of the filtrate was diluted to 100 ml with 0.1 N HCl (for the spectrophotometric method). A 10 ml aliquot of the filtrate was diluted to 100 ml with ethanol (for the voltammetric method). Then the procedure was completed as described under construction of calibration curves.

References

Adams RN (1969) Electrochemistry at Solid Electrodes. Marcell Dekker, New York.

El Yazbi FA, Blaih SM (1993) Spectrophotometric and titrimetric determination of clindamycin hydrochloride in pharmaceutical preparations. Analyst 118: 577–579.

El Yazbi FA, Gazy AA, Mahgoub H, El Sayed MA, Youssef RM (2003) Spectrophotometric and titrimetric determination of nizatidine in capsules. J Pharm Biomed Anal 31: 1027–1034.

El-Hallag I, Hassanien AM, Gaber M, Issa RM (1994) The electrochemical behaviour of some coumarine azo compounds in different pH at mercury electrode. Bull Electrochem 10: 291.

Ferreiros N, Iriarte G, Alonso RM, Jimenez RM, Ortiz E (2006) Validation of a solid phase extraction-high performance liquid chromatographic method for the determination of eprosartan in human plasma. J Chromatogr A 1119: 309–314.

Gonzalez L, Akesolo U, De Jimenez RM, Alonso RM (2002) Application of capillary zone electrophoresis to the screening of some angiotensin II receptor antagonists. Electrophoresis 23: 223–229.

Hammud HH, Ghannoum A, Kabbani A (2006) Electrochemical decomposition of some azo dyes using Pt electrodes. Thermodynamic parameters for methyl red. Bull Electrochem 22: 81–96.

Hillaert S, De Beer TR, De Beer JO, Van den Bossche W (2003) Optimization and validation of a micellar electrokinetic chromatographic method for the analysis of several angiotensin-II-receptor antagonists. J Chromatogr A 984: 135–146.

Jain R, Jain U (1994) Electrochemical investigations on some 1-dinitrophenylarylazopyradoles. Bull Electrochem 10: 297.

Jr. Lundberg DE, Person CR, Knox S, Cyronak MJ (1998) Determination of SK&F (Teveten) in human plasma by reversed-phase high performance liquid chromatography. J Chromatogr B Biomed Sci Appl 707: 328–333.

Ruilope L, Jager B (2003) Eprosartan for the treatment of hypertension. Expert Opin Pharmacother 4: 107–114.

Shusterman NH (1999) Safety and efficacy of Eprosartan, a new angiotensin II receptor blocker. Am Heart J 138: S238–S245.